Control technique for enhancing the stable operation of distributed generation units within a microgrid

Majid Mehrasa[1], Edris Pouresmaeil[2], Hasan Mehrjerdi[3], Bo Nørregaard Jørgensen[2], João P. S. Catalão[4,5,6*]

[1] Young Researchers and Elite Club, Sari Branch, Islamic Azad University, Sari, Iran

[2] Centre for Energy Informatics, Faculty of Engineering, University of Southern Denmark (SDU), Odense, Denmark

[3] Electrical Engineering Department, Qatar University, Doha, Qatar

[4] University of Beira Interior, R. Fonte do Lameiro, Covilha, Portugal

[5] INESC-ID, R. Alves Redol, Lisbon, Portugal

[6] IST, University of Lisbon, Av. Rovisco Pais, Lisbon, Portugal

Abstract: This paper describes a control technique for enhancing the stable operation of distributed generation (DG) units based on renewable energy sources, during islanding and grid-connected modes. The Passivity-based control technique is considered to analyse the dynamic and steady-state behaviours of DG units during integration and power sharing with loads and/or power grid, which is an appropriate tool to analyse and define a stable operating condition for DG units in microgrid technology. The compensation of instantaneous variations in the reference current components of DG units in *ac*-side, and *dc*-link voltage variations in *dc*-side of interfaced converters, are considered properly in the control loop of DG units, which is the main contribution and novelty of this control technique over other control strategies. By using the proposed control technique, DG units can provide the continuous injection of active power from DG sources to the local loads and/or utility grid. Moreover, by setting appropriate reference current components in the control loop of DG units, reactive power and harmonic current components of loads can be supplied during the islanding and grid-connected modes with a fast dynamic response. Simulation results confirm the performance of the control scheme within the microgrid during dynamic and steady-state operating conditions.

Keywords: Microgrid; passivity-based control; distributed generation (DG); grid-connected mode; islanding mode.

* Corresponding Author: João P. S. Catalão, Email: catalao@ubi.pt

Tel: +351-275-329914: Fax: +351-275-329972.

1. Nomenclature

Indices

i	1, 2	$f_j^{*\prime}$	Initial frequency of $i_{cdi} - f_i$ curve
k	3,4, 5	$E_i^{*\prime}$	Initial voltage amplitude of $i_{cqi} - E_i$ curve
w	d, q	i_{nlwj}	Nonlinear loads currents
Variables		$\tilde{i}_{nldj}$	d-axis of nonlinear Load current in harmonic frequency
v_{dci}	*dc*-link voltage	i_{mnldj}	Nonlinear Load current in main frequency
v_{wi}	Voltage at the PCC	i_{llw}	Linear load currents
i_{cwi}	DG current components	R	Radius of $i_{cdi} - i_{cqi}$ curve
i_{fwi}	Currents of capacitor filters	R'	Radius of $P_{ci} - Q_{ci}$ curve
u_{eqwi}	Equivalent switching state functions	(¤, ¨)	Centre of $f_i - E_i$ curve
P_{ci}	Active power of DG	«$_i'$Γ	Small diameter of $f_i - E_i$ curve
Q_{ci}	Reactive power of DG	¥$_i'$Γ	Big diameter of $f_i - E_i$ curve
f_i	Output frequency of DG unit	(~,)	Centre of curve
E_i	Amplitude of voltages at PCC	R_{ci}	Resistance of DG units
$W_{mg}(t)$	Total energy of microgrid system	L_{ci}	Inductance of DG units
$W_{ci}(t)$	Total energy of DG units	C_{dci}	Capacitor of dc link voltages
Δf_i	Frequency deviation of DG units	C_i	Capacitor of filter
ΔE_i	Deviation of voltage amplitudes at the PCC	µ	Grid angular frequency
Δi_{cwi}	deviation of DG currents	«$_i$	Slope of $P_{ci} - f_i$ curve
$\tilde{i}_{avwi}$	Instantaneous variations of DG currents	¥$_i$	Slope of $Q_{ci} - E_i$ curve

$\tilde{v}_{avi}$	Instantaneous variations of *dc*-link voltage	«$_i'$	Slope of $i_{cdi} - f_i$ curve
$\tilde{i}_{refwi}$	Instantaneous variations of DG reference current components	¥$_i'$	Slope of $i_{cqi} - E_i$ curve
i_{refwi}	Reference current values of DG unit	f_i^*	Reference frequency of DG units
v_{refwi}	Reference values of voltages at the PCC	E_i^*	Reference amplitude of voltages at the PCC
v_{refdci}	Reference values of *dc*-link voltages	***Abbreviation***	
P_{refci}	Reference active power of DG units	PCC	Point of Common Coupling
Q_{refci}	Reference reactive power of DG units	DG	Distributed Energy Source
$P_{ci\max}$	Maximum active power of DG units	PI	Proportional-Integral
ΔP_{ci}	Variation of active power in DG units	CC	Capacity Curve
ΔQ_{ci}	Variation of reactive power in DG units	VSC	Voltage Source Converter
Parameters		LPF	Low Pass Filter
R_{dampii}	Series resistance for current state variables	STSs	Static Transfer Switches
R_{dampki}	Series resistance for voltage state variables	BESS	Battery Energy Storage System

2. Introduction

Distributed Generation (DG) technology based on renewable energy sources brings many benefits for electrical power grids regarding the environmental regulation and cost of power generation [1-2]. A systematic structure of DG units forms a microgrid in the power network, which has been proposed to solve the integration problems of single DG units in power system. Proper control of multi DG units in a microgrid can create an independent power network for support of utility grid with loads peak mitigation and enhancement of power quality and reliability of main grid [3-5], regardless of control complexities of DG units in whole system.

Microgrid is more efficient technology in comparison with a single DG unit, concerns on grid reliability and power quality demand. Moreover, microgrid gives many options for optimizing the power of DG units via the combined heat and power, which is one of the most useful strategies for improving the efficiency of whole system.

Different control strategies have been proposed in microgrid to reach an accurate active and reactive power sharing along with remaining at desired values of output voltage magnitude and frequency, in both islanding and grid-connected modes [6-11]. A small signal dynamic model of a microgrid which comprises DG units as synchronous machine and converter-interfaced distributed source is presented in [12]. The model that considers the deviations of main frequency includes: (a) electro-mechanical dynamics of the synchronous machine including exciter and governor systems, (b) dynamics of the voltage source converter (VSC) and its active/reactive power controllers, and (c) dynamic of whole network. A static droop characteristics combined with an adaptive transient droop function in [13] to damp the fluctuations of power sharing controller in DG units. The created adaptive power sharing control technique is used to guarantee the stability of multiple paralleled DG units microgrid at different load sharing. Optimization methods can be used to robust control of microgrid system against the voltage and frequency deviations. In [14], the parameters of droop-control and L1 control theory are optimized by swarm optimization algorithms such that the multiple DGs microgrid operates properly in both grid-connected and islanding modes. A photovoltaic system can be connected into the grid in a single phase microgrid network by using a high-voltage gain switched inductor boost converter, cascaded with a current shaping circuit, followed by a H-bridge converter [15], in order to obtain high boosting gain, lower switching losses, and reduce the ground leakage current. Different control strategies such as charge/discharge control for distributed integration of battery energy storage system (BESS) [16], the improved universal active and reactive power flow controllers for operation of three-phase converters in the virtual power plant environment [17], reactive power sharing controller based on an adaptive voltage droop scheme for the parallel operation of VSC [18], droop control method based on the proper design of a fictitious impedance along with a new restoration control [19], are employed in microgrid to enhance the stable operation of system against any parameter changes, with fast dynamic response. Also in order to smooth the output power of wind turbine to decrease microgrid frequency and voltage fluctuations during the islanding mode, a new fuzzy logic pitch angle controller is designed in [20].

Nyquist criterion with active compensation techniques and admittance-based analysis are applied to an *ac* microgrid in [21]. The proposed compensators are linear with a simple structure and the whole power rating of interfaced-converter is only used for the compensator, regardless of terminated power electronic loads. A spatial repetitive controller can be used to calculate the periodic disturbances of the system for an unbalanced grid voltages and line side inductors in a generalized three phase microgrid, which leads to a current controller improvement technique [22]. Considering a virtual inductor at the output of interfaced converters with online impedance voltage drop effect estimation, potential function based method, decentralized control techniques, and using static synchronous compensator (STATCOM), are other control schemes to reach a stable operation for microgrid [23-26]. In [27], three different topologies, the parallel active topology, the floating topology and the 3-level neutral point clamped (3LNPC) converter topology are used to control a hybrid energy storage system formed by a super capacitor bank and a vanadium redox battery in a microgrid structure. An appropriate control plan is proposed in [28] for charge and discharge of storage devices, to boost the power quality of microgrid, based on storage based DG units. The proposed control plan is employed for compensation of reactive power and harmonic current components of loads.

Several other control techniques have been proposed in concept of microgrid which in most of the presented methods a solution for a serious problem in the power network has been proposed and discussed. In this paper, the authors are introducing a control technique based on the Passivity control technique for defining a stable operating region of DG units in a microgrid system. The impacts of instantaneous variations of reference current components in *ac*-side, and *dc*-voltage variations of capacitor in *dc*-side of interfaced converters in operation of DG units are considered properly, which is the main section regarding the new contribution of this control scheme over the other control algorithms. Contribution of this control technique in microgrid can be introduced as a solution while compensation for the different issues is needed concurrently during the connection of multiple DG units in different operating modes.

The rest of the paper is organized into four sections. Following the introduction, general schematic diagram of the proposed microgrid will be introduced in Section 3 and dynamic and steady-state analysis of the proposed scheme will be elaborated properly. Application of Passivity control technique for the control and stable operation of DG interfacing systems in different operating conditions will be presented in section 4. Moreover, simulation results are performed to demonstrate the efficiency and applicability of the developed control strategy in Section 5. Finally, some conclusions are drawn in Section 6.

3. Dynamic Model Analysis of the Proposed Microgrid Schema

Figure 1 depicts the general configuration of the proposed microgrid model, which is composed by two DG units with local power generation sources and different loads. DG units are isolated and/or connected to the point of common coupling (PCC) through static transfer switches (STSs). Utility grid is connected to the PCC via a static transformer and supplies the grid-connected load until the DG1 change from the isolated mode to the grid-connected mode. In addition, DG1 generates the required active and reactive power for the local load and then is linked to the PCC through STS in a specified time. Both the DG units are regulated to inject their maximum active power during the unexpected load increment during the grid-connected mode.

To draw an appropriate control plan for DG units in microgrid, dynamic equations of the proposed model should be calculated as,

$$\begin{aligned}
&L_{ci}\frac{di_{cdi}}{dt}+R_{ci}i_{cdi}-\mu L_{ci}i_{cqi}+u_{eq_{di}}v_{dci}+v_{di}=0\\
&L_{ci}\frac{di_{cqi}}{dt}+R_{ci}i_{cqi}+\mu L_{ci}i_{cdi}+u_{eq_{qi}}v_{dci}+v_{qi}=0\\
&C_{i}\frac{dv_{di}}{dt}-\mu C_{i}v_{qi}-i_{fdi}=0\\
&C_{i}\frac{dv_{qi}}{dt}+\mu C_{i}v_{di}-i_{fqi}=0\\
&C_{dci}\frac{dv_{dci}}{dt}-u_{eq_{di}}i_{cdi}-u_{eq_{qi}}i_{cqi}-i_{dci}=0
\end{aligned} \tag{1}$$

The capacitance C_i is used to generate sufficient reactive power to fix the magnitude of voltages at PCC in a desired value.

A. Control of voltage magnitude and frequency

In this section, d and q components of injected currents from DG units are employed to predict the changes in magnitude of voltage and frequency, during the different operating modes in the proposed microgrid model. An accurate tracking of voltage magnitude and errors in frequency, based on injected current components from DG units and considering the maximum capacity of their interfaced systems should be employed for the proposed plan to perform a suitable active and reactive power sharing between DG units, loads, and/or utility grid as a controllable and independent power network. According to the two first terms of Eq. (1), switching functions of the interfaced converters in DG units can be obtained as,

$$\begin{aligned} u_{eq_{di}} &= \frac{-1}{v_{dci}}\left(L_{ci}\tilde{i}_{avdi} + R_{ci}i_{cdi} - \omega L_{ci}i_{cqi} + v_{di}\right) \\ u_{eq_{qi}} &= \frac{-1}{v_{dci}}\left(L_{ci}\tilde{i}_{avqi} + R_{ci}i_{cqi} + \omega L_{ci}i_{cdi} + v_{qi}\right) \end{aligned} \tag{2}$$

where $\tilde{i}_{avzi} = \frac{di_{czi}}{dt}$. By substituting (2) in last term of (1), limit area of injected currents from the DG units can be obtained during the dynamic operating condition as,

$$\left(i_{cdi} + \frac{L_{ci}\tilde{i}_{avdi} + v_{di}}{2R_{ci}}\right)^2 + \left(i_{cqi} + \frac{L_{ci}\tilde{i}_{avqi}}{2R_{ci}}\right)^2 = \frac{\left(L_{ci}\tilde{i}_{avdi} + v_{di}\right)^2 + \left(L_{ci}\tilde{i}_{avqi}\right)^2 + \left(i_{dci} - C_{dci}\tilde{v}_{avi}\right)v_{dci}}{4R_{ci}^2} \tag{3}$$

where $\tilde{v}_{avi} = \frac{dv_{dci}}{dt}$ is the average values of instantaneous variations in *dc*-side voltages of interfaced converters. Equation (3) is equation of a circle model as drawn in Fig. 2, which clarifies the capability of DG units for generating or consuming maximum current components, which can be altered through centre of $\left(\alpha,\beta\right) = \left(-\frac{L_{ci}\tilde{i}_{avdi} + v_{di}}{2R_{ci}}, -\frac{L_{ci}\tilde{i}_{avqi}}{2R_{ci}}\right)$ and radius of $R = \sqrt{\frac{\left(L_{ci}\tilde{i}_{avdi} + v_{di}\right)^2 + \left(L_{ci}\tilde{i}_{avqi}\right)^2 + \left(i_{dci} - C_{dci}\tilde{v}_{avi}\right)v_{dci}}{4R_{ci}^2}}$, that are dependent on the parameters of DG units, *dc*-link voltages, variations of reference current components in the control loop of DG units, and voltage at the PCC.

As can be seen, the operating point on the $i_{cdi} - i_{cqi}$ curve can be changed through a current vector as,

$$\sqrt{i_{dx}^2 + i_{qx}^2}\,.e^{jtng^{-1}\left(\frac{i_{qx}}{i_{dx}}\right)} \tag{4}$$

where, $\sqrt{i_{dx}^2 + i_{qx}^2}$ and $tng^{-1}\left(\frac{i_{qx}}{i_{dx}}\right)$ are the magnitude and angle of current component, respectively. With respect to Fig. 2, the maximum and minimum of injected current from the DG units can be calculated as,

$$i_{cd\max} = |R| - |\sim|, i_{cd\min} = -\left(|R| + |\sim|\right), i_{cq\max} = |R| - |\quad| \; and \; i_{cq\min} = -\left(|R| + |\quad|\right) \tag{5}$$

The limited capacity of each DG unit in the proposed microgrid can be determined through (5), which should be considered as an important factor for the proposed control technique. The equations of conventional droop control characteristics can be expressed as,

$$f_i = f_i^* - \text{«}_i\left(P_{ci} - P_{refci}\right) \tag{6}$$

$$E_i = E_i^* - \text{¥}_i\left(Q_{ci} - Q_{refci}\right) \tag{7}$$

In the operating condition, the output active and reactive power of DG units are equal to $P_{ci} = v_{di}i_{cdi}$ and $Q_{ci} = -v_{di}i_{cqi}$. By substituting these equations into (6) and (7) and doing the associated mathematical calculations, characteristic equation of $i_{cdi} - f_i$ and $i_{cqi} - E_i$ can be obtained as,

$$f_i = f_i^{*\prime} - \text{«}_i' i_{cdi} \tag{8}$$

$$E_i = E_i^{*\prime} + \text{¥}_i' i_{cqi} \tag{9}$$

where $f_i^{*\prime} = f^* + «_i P_{refci}$, $E_i^{*\prime} = E^* + ¥_i Q_{refci}$, $«_i' = «_i \times v_{di}$ and $¥_i' = ¥_i \times v_{di}$. Equations (8) and (9) verify that the voltage magnitude and frequency of DG units in the microgrid can be controlled through current components of DG units. On the other hand, in order to operate near the steady-steady points in dynamic operating conditions, the appropriate selection of reference current components in the control loop of DG units lead to minimize deviation of voltage magnitude and frequency from their desired values. The characteristic curves $i_{cdi} - i_{cqi}$, $i_{cdi} - f_i$, and $i_{cqi} - E_i$ are shown in Fig. 3. As indicated in this figure, during the islanding mode DG generates current in d-axis and consumes current in q-axis, which is associated with the capacitor C of filter for regulating the magnitude of voltage at a desired value. When DG moves from the islanding mode to the grid-connected mode, $i_{cdi} - i_{cqi}$ curve converts to a larger circle due to the current variations in which DG unit is responsible to generate q-axis current and its maximum capacity of d-axis current for the grid ($i_{cdi2} \rightarrow i_{c\dim ax}$). As shown in Fig. 3.b, during the grid-connected mode, frequency of DG unit reaches to the reference value and then for provide the maximum amplitude of d-axis current, $i_{cdi} - f_i$ curve shifts to the right-up with constant slope and the current difference of Δi_{cdi} is compensated to approaches to i_{cdi2}. Moreover, according to Fig. 3.c, the $i_{cqi} - E_i$ curve moves to the left-up with the same slope to keep its desired voltage magnitude and generate the reactive power which is needed to supply the loads.

B. Control of voltage magnitude and frequency through $P_{ci} - Q_{ci}$ curve

Changes in injected active and reactive power from DG units can be considered as criteria to track the voltage magnitude and frequency errors, and subsequently construct an appropriate controller to decrease these errors. By multiplying v_{di}^2 to (3), the equation of capability curve (CC) for a DG unit can be achieved as,

$$\left(P_{ci}+\frac{L_{ci}\tilde{i}_{avdi}v_{di}+v_{di}^2}{2R_{ci}}\right)^2+\left(Q_{ci}-\frac{L_{ci}\tilde{i}_{avqi}v_{di}}{2R_{ci}}\right)^2=\frac{\left(L_{ci}\tilde{i}_{avdi}v_{di}+v_{di}^2\right)^2+\left(L_{ci}\tilde{i}_{avqi}v_{di}\right)^2+\left(i_{dci}-C_{dci}\tilde{v}_{avi}\right)v_{dci}v_{di}^2}{4R_{ci}^2} \tag{10}$$

where,

$$c'=\left(-\frac{L_{ci}\tilde{i}_{avdi}v_{di}+v_{di}^2}{2R_{ci}},\frac{L_{ci}\tilde{i}_{avqi}v_{di}}{2R_{ci}}\right),\ R'=\sqrt{\frac{\left(L_{ci}\tilde{i}_{avdi}v_{di}+v_{di}^2\right)^2+\left(L_{ci}\tilde{i}_{avqi}v_{di}\right)^2+\left(i_{dci}-C_{dci}\tilde{v}_{avi}\right)v_{dci}v_{di}^2}{4R_{ci}^2}}$$

The CC, $P_{ci}-f_i$ and $Q_{ci}-E_i$ droop control characteristic curves of DG are shown in Fig. 4. DG unit with the capability curve of CC1 is in islanding mode and provides active power and consumes reactive power related to the load consumption and C filter. Also, up and low limits of $P_{ci}-f_i$ and $Q_{ci}-E_i$ curves in islanding state can be determined through the CC1.

In order to supply the reactive power of loads and inject the maximum active power of DG unit to the grid during the grid-connected mode, the capability curve of DG unit is changed to CC2 with operating point of $\left(P_{ci2},Q_{ci2}\right)$. Since, in grid connected mode, the voltage magnitude and frequency of DG unit is matched with grid ones, $P_{ci}-f_i$ and $Q_{ci}-E_i$ curves get into red curves as indicated in Fig. 4. In addition, their maximum and minimum value changes with respect to the capability curve of CC2. According to CC in Fig. 4, the maximum and minimum active and reactive powers of DG unit are equal to,

$$P_{c\max}=\left|R'\right|-\left|v_{di}^2\sim\right|,P_{c\min}=-\left(\left|R'\right|+\left|v_{di}^2\sim\right|\right),Q_{c\max}=\left|R'\right|+\left|v_{di}^2\quad\right| and\ Q_{c\min}=-\left(\left|R'\right|-\left|v_{di}^2\quad\right|\right) \tag{11}$$

C. Control of voltage magnitude and frequency through $f_i - E_i$ *curve*

A comprehensive recognition of operating region, associated with simultaneous changes in voltage magnitude and frequency can be enhanced in both dynamic and steady-state operating conditions, in order to evaluating the ability of microgrid for supplying the voltage magnitude and frequency changes during different conditions of DG units and utility grid. In addition, the accurate operation of active and reactive power sharing technique can be effectively improved with synchrony trace of voltage magnitude and frequency during presence of dynamic changes in whole system. According to (3), the $i_{cdi} - i_{cqi}$ curve in steady-state can be written as,

$$\left(i_{refdi} + \frac{L_{ci}\tilde{i}_{refdi} + v_{refdi}}{2R_{ci}}\right)^2 + \left(i_{refqi} + \frac{L_{ci}\tilde{i}_{refqi}}{2R_{ci}}\right)^2 = \frac{\left(L_{ci}\tilde{i}_{refdi} + v_{refdi}\right)^2 + \left(L_{ci}\tilde{i}_{refqi}\right)^2 + I_{dci}v_{refdci}}{4R_{ci}^2} \quad (12)$$

d and q components of currents injected from DG units are equal to,

$$i_{cdi} = i_{refdi} + \Delta i_{cdi} \quad (13)$$

$$i_{cqi} = i_{refqi} + \Delta i_{cqi} \quad (14)$$

With respect to (8) and (9), desired values of d and q components of injected current from the DG unit can be obtained as,

$$i_{refdi} = \frac{f_i - f_i^{*\prime}}{-\text{«}_i'} - \frac{\Delta f_i}{-\text{«}_i'} \quad (15)$$

$$i_{refqi} = \frac{E_i - E_i^{*\prime}}{-\text{¥}_i'} - \frac{\Delta E_i}{-\text{¥}_i'} \quad (16)$$

By substituting (15) and (16) into (12), (17) can be expressed as,

$$\left(\frac{f_i - f_i^*}{-\mu_i'} - \frac{\Delta f_i}{-\mu_i'} + \frac{L_{ci}\tilde{i}_{refdi} + v_{refdi}}{2R_{ci}}\right)^2 + \left(\frac{E_i - E_i^*}{-\gamma_i'} - \frac{\Delta E_i}{-\gamma_i'} + \frac{L_{ci}\tilde{i}_{refqi}}{2R_{ci}}\right)^2 = \frac{\left(L_{ci}\tilde{i}_{refdi} + v_{refdi}\right)^2 + \left(L_{ci}\tilde{i}_{refqi}\right)^2 + I_{dci}v_{refdci}}{4R_{ci}^2} \tag{17}$$

Equation (17) can be considered equivalent as,

$$\frac{\left(f_i - \text{¤}\right)^2}{\text{«}_i'^2} + \frac{\left(E_i - \text{¨}\right)^2}{\text{¥}_i'^2} = \Gamma^2 \tag{18}$$

where,

$$\phi = \frac{2R_{ci}f_i^* + 2R_{ci}\Delta f_i + L_{ci}\tilde{i}_{refdi}\mu_i' + v_{refdi}\mu_i'}{2R_{ci}},\ \varphi = \frac{2R_{ci}E_i^* + 2R_{ci}\Delta E_i + L_{ci}\tilde{i}_{refqi}\gamma'}{2R_{ci}},$$

$$\Gamma = \sqrt{\frac{\left(L_{ci}\tilde{i}_{refdi} + v_{refdi}\right)^2 + \left(L_{ci}\tilde{i}_{refqi}\right)^2 + I_{dci}v_{refdci}}{4R_{ci}^2}}$$

Equation (18) is equation of an ellipse with centre of $\left(\text{¤}, \text{¨}\right)$ and two small and big diameters of $\text{«}_i'\Gamma$ and $\text{¥}_i'\Gamma$, and called as $f_i - E_i$ curve in DG technology. Each operating point in $f_i - E_i$ curve can be specified through a vector with amplitude of $\text{£}_i = \sqrt{f_i^2 + E_i^2}$ and angle of $\text{¯}_i = \tan^{-1}\left(E_i / f_i\right)$. The dashed sections illustrate the ability of DG unit in generating different positive voltage magnitude and frequency, which are needed for various microgrid systems. In addition, (18) confirms that different characteristics of $f_i - E_i$ curve can be altered through the parameters of DG unit, slopes of the $i_{cdi} - f_i$ and $i_{cqi} - E_i$ curves, variations of DG unit currents in the steady-state, voltage magnitude, and frequency deviations.

D. Synchrony consideration of active-reactive power and voltage magnitude-frequency curve

DG units in microgrid system should be able to generate active and reactive power of load and also reach to the desired voltage magnitude and frequency after an acceptable transient time. The $P_{ci} - Q_i$ and $f_i - E_i$ curves of each DG unit include specifications and areas, which can be used to demonstrate whether the DG unit can supply active and reactive power that are planned in a microgrid system and approach to the reference values of voltage magnitude and frequency.

As discussed in section C, with changes in the centre and diameters of $f_i - E_i$ curve, DG unit can be matched with magnitude of desired voltage and frequency, which leads to increment in the covered area through $P_{ci} - Q_i$ curve. The proposed microgrid model can be operate in a stable condition, if both the *P-Q* and *E-f* curves of loads located inside the *P-Q* and *E-f* curves of DG unit/units.

4. Proposed Control Technique

The proposed control strategy in this paper is based on Passivity Control theory [29]. The proposed control technique present a proper procedure for tracing of reference current components in the control loop of DG units in whole microgrid system, in order to regulate the output frequency and voltage magnitude deviations of DG units and keep a zero value for the harmonic components and reactive power injected through the utility grid during presence of nonlinear loads.

A. Passivity-based control description

A passive system is defined as a network, which consumes energy and is not able to generate its own energy in different conditions. If $P_c(t)$ is considered as the power of passive system, energy of whole system can be calculated as,

$$W_c(t)=\int_{-\infty}^{t}P_c(t)\,dt=\int_{-\infty}^{0}P_c(t)\,dt+\int_{0}^{t}P_c(t)\,dt\geq 0 \tag{19}$$

The first term in last part of (19) demonstrates the initial value of energy, which is equal to zero value in a passive system. In order to do the Passivity analysis in proposed microgrid model, Eq. (1) should be described as below matrix,

$$m_{cdqi}\dot{i}_{cdqi}+r_{cdqi}i_{cdqi}+w_{cdqi}i_{cdqi}+u_{cdqi}i_{cdqi}+I_{cdqi}=0 \tag{20}$$

where, $m_{cdqi}, r_{cdqi}, w_{cdqi}, u_{cdqi}$ and I_{cdqi} are given in Appendix I. The error state variables of close control loop in the proposed model are defined as,

$$e_{cdqi}=i_{cdqi}-i_{refcdqi}=\begin{bmatrix}e_{1i} & e_{2i} & e_{3i} & e_{4i} & e_{5i}\end{bmatrix}^T= \begin{bmatrix}i_{cdi}-i_{refdi} & i_{cqi}-i_{refqi} & v_{di}-v_{refdi} & v_{qi}-v_{refqi} & v_{dci}-v_{refdci}\end{bmatrix}^T \tag{21}$$

The state-space model of the proposed microgrid based on the error and reference state variables can be achieved according to (20) and (21) as,

$$m_{cdqi}\dot{e}_{cdqi}+r_{cdqi}e_{cdqi}+w_{cdqi}e_{cdqi}+u_{cdqi}e_{cdqi}=-I_{cdqi}-\left(m_{cdqi}\dot{i}_{refcdqi}+r_{cdqi}i_{refcdqi}+w_{cdqi}i_{refcdqi}+u_{cdqi}i_{refcdqi}\right) \tag{22}$$

The first step in the Passivity-based control model is injecting suitable series damping resistances to each variable of DG units, in order to make the total saved energy of microgrid equal to the zero value, or reach to a finite value in the various routes of state variables in the microgrid model. The damping resistance matrix $r_{dampi}=R_{dampi}I_{5\times 5}$ is added in two sides of (22);

consequently, the close loop dynamic model of system errors based on Passivity method can be obtained as,

$$m_{cdqi}\dot{e}_{cdqi}+\left(r_{cdqi}+R_{dampi}I_{5\times5}\right)e_{cdqi}+w_{cdqi}e_{cdqi}+u_{cdqi}e_{cdqi}= \\ -I_{cdqi}-\left(m_{cdqi}\dot{i}_{refcdqi}+r_{cdqi}i_{refcdqi}+w_{cdqi}i_{refcdqi}+u_{cdqi}i_{refcdqi}-R_{dampi}I_{5\times5}.e_{cdqi}\right) \tag{23}$$

In addition, the Passivity-based control strategy should force the variables of proposed model to follow their desired values. To reach this goal, the right side of (23) should be equal to zero value as,

$$m_{cdqi}\dot{e}_{cdqi}+\left(r_{cdqi}+R_{dampi}I_{5\times5}\right)e_{cdqi}+w_{cdqi}e_{cdqi}+u_{cdqi}e_{cdqi}=0 \tag{24}$$

In order to verify the precision of (24), total reserved energy of each DG unit should be defined as,

$$W_{ci}\left(t\right)=\frac{1}{2}L_{ci}e_{1i}^{2}+\frac{1}{2}L_{ci}e_{2i}^{2}+\frac{1}{2}C_{i}e_{3i}^{2}+\frac{1}{2}C_{i}e_{4i}^{2}+\frac{1}{2}C_{dci}e_{5i}^{2} \tag{25}$$

Then, the direct Lyapunov control theory can be used to demonstrate the capability of Passivity control technique for minimizing the total saved energy of the whole proposed model, which is called as energy shaping in final step of this strategy. Derivative of (25) can be calculated as,

$$\dot{W}_{ci}\left(t\right)=L_{ci}e_{1i}\dot{e}_{1i}+L_{ci}e_{2i}\dot{e}_{2i}+C_{i}e_{3i}\dot{e}_{3i}+C_{i}e_{4i}\dot{e}_{4i}+C_{dci}e_{5i}\dot{e}_{5i}=e_{cdqi}^{T}m_{cdqi}\dot{e}_{cdqi} \tag{26}$$

With respect to (24), the matrix term of (26) can be rewritten as,

$$\dot{W}_{ci}\left(t\right)=-e_{cdqi}^{T}m_{cdqi}\left[m_{cdqi}^{-1}\left(\left(r_{cdqi}+R_{dampi}I_{5\times5}\right)e_{cdqi}+w_{cdqi}e_{cdqi}+u_{cdqi}e_{cdqi}\right)\right] \\ \dot{W}_{ci}\left(t\right)=-\left(\underline{e_{cdqi}^{T}\left(r_{cdqi}+R_{dampi}I_{5\times5}\right)e_{cdqi}}+e_{cdqi}^{T}w_{cdqi}e_{cdqi}+e_{cdqi}^{T}u_{cdqi}e_{cdqi}\right) \tag{27}$$

By adding the suitable damping resistances, the underlined part of (27) can be much larger than other terms, consequently (27) can be rewritten as,

$$\dot{W}_{ci}\left(t\right) = -e_{cdqi}^{T}\left(r_{cdqi} + R_{dampi} I_{5\times5}\right)e_{cdqi} \tag{28}$$
$$\dot{W}_{ci}\left(t\right) = -\left(R_{ci} + R_{damp1i}\right)e_{1i}^{2} - \left(R_{ci} + R_{damp2i}\right)e_{2i}^{2} - R_{damp3i}^{-1}e_{3i}^{2} - R_{damp4i}^{-1}e_{4i}^{2} - R_{damp5i}^{-1}e_{5i}^{2} \le 0$$

Equation (28) verifies the energy shaping process of Passivity-based control technique for DG units. In addition, (28) confirms that the state variables of close control loop are able to trace their reference values with a fast dynamic response, and an asymptotical global stability will be achieved for the whole system. Since the proposed microgrid model is consisted of two DG units; then,

$$W_{mg}\left(t\right) = W_{c1}\left(t\right) + W_{c2}\left(t\right) \tag{29}$$

According to (29), the proposed microgrid model will be passive if two DG units are passive. Total saved energy of microgrid is sum of the total energies of each DG unit, which leads to a passive microgrid model with a stable behaviour according to the passive and stability criteria in DG technology.

dc-link voltage regulation of DG units is an important issue in the proposed control plan, to force the variables of microgrid to reach their reference values with fast dynamic response and minimum errors. The Passivity-based model in the proposed scheme should be able to make a stable zero dynamic for input voltage in the close control loop. According to (23) and (24), a set of Passivity-based state equation can be obtained through a matrix description as,

$$m_{cdqi}\dot{i}_{refcdqi} + r_{cdqi}i_{refcdqi} + w_{cdqi}i_{refcdqi} + u_{cdqi}i_{refcdqi} - R_{dampi}I_{5\times5}.e_{cdq} + I_{cdqi} = 0 \tag{30}$$

By substituting the defined parameters from Appendix I in (30), (31) can be expressed as,

$$
\begin{aligned}
&L_{ci}\frac{di_{refdi}}{dt}+R_{ci}i_{refdi}-\mu L_{ci}i_{refqi}+v_{refdi}+u_{eq_{di}}v_{refdci}-R_{damp1i}\left(i_{cdi}-i_{refdi}\right)=0\\
&L_{ci}\frac{di_{refqi}}{dt}+R_{ci}i_{refqi}+\mu L_{ci}i_{refdi}+v_{refqi}+u_{eq_{qi}}v_{refdci}-R_{damp2i}\left(i_{cqi}-i_{refqi}\right)=0\\
&C_{i}\frac{dv_{refdi}}{dt}-\mu C_{i}v_{refqi}-R_{damp3i}^{-1}\left(v_{di}-v_{refdi}\right)-i_{fdi}=0\\
&C_{i}\frac{dv_{refqi}}{dt}+\mu C_{i}v_{refdi}-R_{damp4i}^{-1}\left(v_{qi}-v_{refqi}\right)-i_{fqi}=0\\
&C_{dci}\frac{dv_{refdci}}{dt}-u_{eq_{di}}i_{refdi}-u_{eq_{qi}}i_{refqi}-R_{damp5i}^{-1}\left(v_{dci}-v_{refdci}\right)-i_{dci}=0
\end{aligned}
\qquad (31)
$$

According to (31), switching state functions of DG units can be obtained as,

$$u_{eq_{di}}=\frac{-1}{v_{refdci}}\left(L_{ci}\tilde{i}_{refdi}+R_{ci}i_{refdi}-\mu L_{ci}i_{refqi}+v_{refdi}-R_{damp1i}\left(i_{cdi}-i_{refdi}\right)\right) \qquad (32)$$

$$u_{eq_{qi}}=\frac{-1}{v_{refdci}}\left(L_{ci}\tilde{i}_{refqi}+R_{ci}i_{refqi}+\mu L_{ci}i_{refdi}+v_{refqi}-R_{damp2i}\left(i_{cqi}-i_{refqi}\right)\right) \qquad (33)$$

By substituting (32) and (33) in the last term of (31), zero dynamic equation of *dc*-link voltage for each DG unit can be obtained as,

$$
\begin{aligned}
C_{dci}\frac{dv_{refdci}}{dt}=&\frac{-i_{refdi}}{v_{refdci}}\left(L_{ci}\tilde{i}_{refdi}+R_{ci}i_{refdi}-\omega L_{ci}i_{refqi}+v_{refdi}+-R_{damp1i}\left(i_{cdi}-i_{refdi}\right)\right)\\
&-\frac{i_{refqi}}{v_{refdci}}\left(L_{ci}\tilde{i}_{refqi}+R_{ci}i_{refqi}+\omega L_{ci}i_{refdi}+v_{refqi}-R_{damp2i}\left(i_{cqi}-i_{refqi}\right)\right)+R_{damp5i}^{-1}\left(v_{dci}-v_{refdci}\right)+i_{dci}
\end{aligned}
\qquad (34)
$$

Since the steady-state variables of DG units should be able to reach their reference values in the proposed controller procedure ($e_i\to 0\left(i=1,\ldots,5\right)$), (34) can be rewritten as,

$$\frac{dv_{refdci}}{dt}=\frac{-R_{ci}i_{refdi}^{2}-R_{ci}i_{refqi}^{2}-\left(L_{ci}\tilde{i}_{refdi}+v_{refdi}\right)i_{refdi}-\left(L_{ci}\tilde{i}_{refqi}+v_{refqi}\right)i_{refqi}+v_{refdci}i_{dci}}{C_{dci}v_{refdci}} \qquad (35)$$

By imposing zero into (35),

$$\frac{dv_{refdci}}{dt}=0 \Rightarrow v_{refdci}i_{dci}=R_{ci}i_{refdi}^{2}+R_{ci}i_{refqi}^{2}+\left(L_{ci}\tilde{i}_{refdi}+v_{refdi}\right)i_{refdi}+\left(L_{ci}\tilde{i}_{refqi}+v_{refqi}\right)i_{refqi} \tag{36}$$

Equation (36) demonstrates, the input power is equal to sum of dissipated power in output resistances and inductances in DG units, and also emerged output power as three phase PCC voltages. Therefore, the zero dynamic of input voltage can be obtained through (36) as,

$$v_{refdci}=\frac{R_{ci}i_{refdi}^{2}+R_{ci}i_{refqi}^{2}+\left(L_{ci}\tilde{i}_{refdi}+v_{refdi}\right)i_{refdi}+\left(L_{ci}\tilde{i}_{refqi}+v_{refqi}\right)i_{refqi}}{i_{dci}} \tag{37}$$

Equation (37) demonstrates a zero dynamic value for dc-link voltage in each DG unit, and confirms that they can trace the reference values, precisely.

B. Reference currents determination

Proper injection of current components from the DG units to the loads and/or grid during the grid-connected or islanding modes decreases the magnitude of output voltage and frequency deviations in a suitable level, regardless of achieving to accurate active and reactive power sharing. DG units are employed to compensate all the harmonic current components and reactive power of nonlinear loads, along with injection of maximum available active power at the fundamental frequency. To reach these goals, reference current components in the control loop of DG units should be defined as,

$$\begin{aligned} i_{nld1}&=i_{mnld1}+\tilde{i}_{nld1}\\ i_{nld2}&=i_{mnld2}+\tilde{i}_{nld2} \end{aligned} \tag{38}$$

DG unit I is responsible to generate the harmonic current components of nonlinear load I and injects its maximum active power based on the capacity of interfaced converter. Also, DG unit I is installed to provide both active and reactive power for the linear loads. If $P_{nl1\max}$ and $P_{ll\max}$ are the maximum active power for nonlinear load I and linear load respectively, the d component of current for unit I should be equal to,

$$i_{cd1} = \begin{cases} i_{nld1} + i_{lld} & if\ P_{c1\max} = P_{nl1\max} + P_{ll\max} \\ \tilde{i}_{nld1} + \dfrac{P_{c1\max}}{v_m} & if\ P_{c1\max} > P_{nl1\max} + P_{ll\max}\ or\ P_{c1\max} < P_{nl1\max} + P_{ll\max} \end{cases} \tag{39}$$

The same scenario is assumed for DG unit II; then,

$$i_{cd2} = \begin{cases} i_{nld2} & if\ P_{c2\max} = P_{nl2\max} \\ \tilde{i}_{nld2} + \dfrac{P_{c2\max}}{v_m} & if\ P_{c2\max} > P_{nl2\max}\ or\ P_{c2\max} < P_{nl2\max} \end{cases} \tag{40}$$

On the other hand, the whole reactive power, which is drawn through linear and nonlinear loads should be compensated via DG units. Moreover, the reactive power of each DG units can be adjusted by employing its current at q-axis. Therefore,

$$\begin{aligned} i_{cq1} &= i_{nlq1} + i_{llq} \\ i_{cq2} &= i_{nlq2} \end{aligned} \tag{41}$$

Equation (41) demonstrates that reactive power of loads are supplied through the DG units. The overall scheme of reference current generation is shown in Fig. 5. As can be seen, the harmonic contents of nonlinear load currents are extracted by use of low pass filter (LPF). Also, proportional integral (PI) controllers are used to minimize the errors between the actual and reference values.

5. Results and Discussions

Figure 6 illustrates the general schematic diagram of the proposed model included by Passivity-based control strategy for microgrids. The proposed scheme is simulated through the MATLAB/Simulink and will be evaluated in both the dynamic and steady-state operating conditions. The following scenarios are planned to assess the dynamic and steady-state operations of the proposed control technique in microgrid, with the aim of proper power sharing and also suitable voltage and frequency regulation. First, nonlinear load I is connected to the utility grid and drawn nonlinear currents from the utility source. This process is continued until t=0.1 sec, while DG unit I is connected to the grid. During this period, DG unit II supplies the nonlinear load II in isolated mode. At t=0.2 sec, DG unit II and linear load are synchronously linked to the utility grid. Both DG units are employed to inject their maximum active power in grid-connected mode and compensate all the reactive power requested from the loads. Also, STSs are employed to change DG unit conditions and load connection. The parameter values of grid, loads, and DG units are given in Appendix II.

A. Active and Reactive Power Sharing Assessment

The active power sharing of DG units during presence of linear and nonlinear loads in the microgrid is depicted in Fig. 7. Fig. 7.a indicates the active power of DG unit I, nonlinear load I, and utility grid. As can be seen from Fig. 7.a, before connection of DG unit I to the grid, power of nonlinear load I is entirely provided through utility grid. But, after connection of DG unit I to the grid (t=0.1 sec), the maximum active power of DG unit I is injected to the utility grid, which is in both fundamental and harmonic frequencies.

In addition, Fig. 7.a illustrates that the rest of available active power in the fundamental frequency (around 9kW), is injected from DG unit I to the grid in time interval $0.1s<t<0.2s$. Fig. 7.b indicates the active power of DG unit II, nonlinear load II, and linear load. As depicted in this figure, DG unit II generates the only required active power of nonlinear load II during the islanding mode. After the connection of DG unit II and linear load to the grid at t=0.2 sec, DG unit II is adjusted to generates its maximum active power in the main frequency, which supply all active power of nonlinear load II. The rest of active power is injected to the utility grid; then, linear load draws the active power from the grid. As depicted in Fig. 7.a, the value of injected active power to the grid reaches around 18 kW in the time interval $0.2s<t<0.3s$.

Reactive power sharing of the proposed microgrid model are shown in Fig. 7.c and Fig. 7.d during dynamic and steady-state operating conditions. Fig. 7.c demonstrates the reactive power of DG unit I, nonlinear load I, and grid for the defined plan. As indicated in this figure, before connection of DG unit I to the grid, all the reactive power in both main and harmonic frequencies are supplied by utility grid. But, after connection of DG unit I to the grid at t=0.1 sec, all the reactive power components are injected through DG unit I; then, utility grid is free of any harmonic frequencies and reactive power components. Moreover, during connection of linear load at the PCC in t=0.2 sec, DG unit I is ready to compensate the additional reactive power; thus, generated reactive power through the grid remains in zero value.

Fig. 7.d illustrates the reactive power sharing between the DG unit II, nonlinear load II, and linear load. As indicated in this figure, before connection of DG unit II, this unit consumes the reactive power generated through the capacitance of filter (C) in order to keep a constant and balanced sinusoidal voltage at the PCC. Consequently, reactive power of nonlinear load II is

generated through the capacitor filter. The exact reactive power of nonlinear load II is provided after connection of DG unit II to the grid.

B. Voltage magnitude and frequency regulation

The frequency variations of DG units and utility grid during whole simulation time are shown in Fig. 8.a. As can be seen from this figure, the grid frequency remains constant at f=50 Hz. However, the output frequency of DG unit I swings in an acceptable ranges with maximum deviation about $\Delta f = 0.004$ Hz and the output frequency of DG unit II reaches to its steady-state values around f=50.022 after t=0.22 sec. General evaluation of Fig. 8.a shows that the proposed control method keeps the frequency of the proposed microgrid at the main frequency. The voltage magnitude of DG units and grid are illustrated in Fig. 8.b. According to Fig. 8.b, after connection of DG unit I to the grid, the output voltage magnitude of DG reaches to its desired value after a short transient time. Also DG unit II keeps its output voltage magnitude in a desired value by using the reactive properties of capacitor filter, and after connection of DG unit II, this voltage traces the grid voltage magnitude after short fluctuations.

C. Harmonic Compensation Analysis

The DG units' current regulation ability of the proposed control strategy with the purposes of harmonic compensation and maximum current injection is investigated in this section. The DG units, grid, nonlinear and linear loads currents in phase "a" are illustrated in fig.9. As it can be seen in this figure, after DG I connection to the grid at t=0.1 sec, the grid current becomes sinusoidal and has the phase difference of 180 degrees with the voltage grid. Thus, the obtained grid current proves that the DG I unit performs completely its three responsibilities toward the grid and nonlinear load I as 1) complete reactive power compensation 2) the different harmonic components compensation of nonlinear load I 3) the injection of the rest of active power of DG I at fundamental frequency to grid. With the synchronous connection of

DG II and linear load to the grid at t=0.2, the grid current reaches the higher amplitude with the same former phase difference toward its respective grid voltage. It shows that the DG II is able to inject its remaining active power at the fundamental frequency to the grid. In addition to this, the harmonic and reactive power compensation duties with the presence of the nonlinear II and linear loads are completely accomplished by the DG II.

The harmonic spectrum of the nonlinear loads and grid currents are depicted in fig.10. According to this figure, before DG I connection, the THD and harmonic spectrum of the grid current is equal to the one for nonlinear load I. After DG I connection, the THD of the grid current is noticeably decreased to 1% with the harmonic components shown in fig.10.b. On the other hand, after DG II connection, the grid current THD remains at the same value of 1% with a significant larger magnitude, which is due to receiving more active power at main frequency.

6. Conclusion

A Passivity-based control technique has been presented in this paper for the stable operation of DG units during grid-connected and islanding modes in microgrid technology. The compensation of instantaneous variations in the reference current components of each DG unit in *ac*-side and *dc*-voltage variations in *dc*-side of the interfaced converters have been considered properly, as the main contribution and novelty of the proposed control strategy in microgrid technology. Simulation results confirmed that, by the utilization of the proposed control technique, DG units can provide the continuous injection of active power from DG sources to the loads and utility grid. Furthermore, the proposed control method has a small transient state and fast dynamic response to provide the reactive power and harmonic current components of nonlinear loads; then, fast tracking of reference voltage magnitude and frequency. The proposed control method can be used for the integration of different types of DG units based on renewable energy sources to supply the local loads and as a power quality enhancement device in a custom power distribution grid.

Appendix 1:

$$m_{cdqi}=\begin{bmatrix} L_{ci} & 0 & 0 & 0 & 0 \\ 0 & L_{ci} & 0 & 0 & 0 \\ 0 & 0 & C_{fi} & 0 & 0 \\ 0 & 0 & 0 & C_{fi} & 0 \\ 0 & 0 & 0 & 0 & C_{dci} \end{bmatrix}, r_{cdqi}=\begin{bmatrix} R_{ci} & 0 & 0 & 0 & 0 \\ 0 & R_{ci} & 0 & 0 & 0 \\ 0 & 0 & 0 & 0 & 0 \\ 0 & 0 & 0 & 0 & 0 \\ 0 & 0 & 0 & 0 & 0 \end{bmatrix}, I_{cdqi}=\begin{bmatrix} 0 \\ 0 \\ -i_{fdi} \\ -i_{fqi} \\ -I_{dci} \end{bmatrix}$$

$$w_{cdqi}=\begin{bmatrix} 0 & -\mu L_{ci} & 1 & 0 & 0 \\ \mu L_{ci} & 0 & 0 & 1 & 0 \\ 0 & 0 & 0 & -\mu C_{fi} & 0 \\ 0 & 0 & \mu C_{fi} & 0 & 0 \\ 0 & 0 & 0 & 0 & 0 \end{bmatrix}, u_{cdqi}=\begin{bmatrix} 0 & 0 & 0 & 0 & u_{eqdi} \\ 0 & 0 & 0 & 0 & u_{eqqi} \\ 0 & 0 & 0 & 0 & 0 \\ 0 & 0 & 0 & 0 & 0 \\ -u_{eqdi} & -u_{eqqi} & 0 & 0 & 0 \end{bmatrix}$$

Appendix 2:

$v_{dci}=1400 volt$, $R_{c1}=R_{c2}=0.1\Omega$, $L_{c1}=L_{c2}=45mH$, $f_{si}=10kHz$, $v_s=380volt$, $L_g=0.1mH$, $R_g=0.1\Omega$

$R_{damp11}=R_{damp12}=8\Omega, R_{damp21}=R_{damp22}=20\Omega$

Nonlinear load I: 3-phase diode rectifier with a resistance-inductance output load of $25+j3.14\Omega$

Nonlinear load II: 3-phase diode rectifier with a resistance-inductance output load of $35+j4.71\Omega$

Linear load $P_{ll}=2.5kW, Q_{ll}=4.5kVAR$

Acknowledgements

This work was supported by FEDER funds (European Union) through COMPETE, and by Portuguese funds through FCT, under Projects FCOMP-01-0124-FEDER-020282 (Ref. PTDC/EEA-EEL/118519/2010) and UID/CEC/50021/2013. Also, the research leading to these results received funding from the EU Seventh Framework Programme FP7/2007–2013 under grant agreement no. 309048.

References

[1] Mehrasa, M., Pouresmaeil, E., Catalao, J.P.S.: 'Direct Lyapunov Control Technique for the Stable Operation of Multilevel Converter-Based Distributed Generation in Power Grid'. IEEE Journal of Emerging and Selected Topics in Power Electronics, 2014, 4, (2), pp. 931-941.

[2] Pouresmaeil, E., Mehrasa, M., Catalão, J.P.S. 'A Multifunction Control Strategy for the Stable Operation of DG in Smart Grids'. IEEE Trans. on Smart Grid, 2014, 6, (2), pp. 598-607.

[3] Rezaei, N., Kalantar, M.: 'Smart microgrid hierarchical frequency control ancillary service provision based on virtual inertia concept: An integrated demand response and droop controlled distributed generation framework'. Energy Conversion and Management, 2015, 92, pp. 287-301.

[4] Mazidi, M., Zakariazadeh, A., Jadid, S., Siano, P.: 'Integrated scheduling of renewable generation and demand response programs in a microgrid'. Energy Conversion and Management, 2014, 86, pp. 1118-1127.

[5] Rezaei, N., Kalantar, M.: 'Economic–environmental hierarchical frequency management of a droop-controlled islanded microgrid'. Energy Conversion and Management, 2014, 88, pp. 498-515.

[6] Koohi-Kamali, S., Rahim, N.A., Mokhlis, H.: 'Smart power management algorithm in microgrid consisting of photovoltaic, diesel, and battery storage plants considering variations in sunlight, temperature, and load'. Energy Conversion and Management, 2014, 84, pp. 562-582.

[7] Hossain, E., Kabalci, E., Bayindir, R., Perez, R.: 'Microgrid testbeds around the world: State of art'. Energy Conversion and Management, 2014, 86, 132-153.

[8] Marzband, M., Sumper, A., Domínguez-García, J.L., Gumara-Ferret, R.: 'Experimental validation of a real time energy management system for microgrids in islanded mode using a local day-ahead electricity market and MINLP'. Energy Conversion and Management, 2013, 76, 314-322.

[9] Gabbara, H.A., Abdelsalama, A.A.: 'Microgrid energy management in grid-connected and islanding modes based on SVC'. Energy Conversion and Management, 2014, 86, (1), pp. 964–972.

[10] Kamel, R.M.: 'Effect of wind generation system types on Micro-Grid (MG) fault performance during both standalone and grid connected modes'. Energy Conversion and Management, 2014, 79, (1), pp. 232–245.

[11] Pouresmaeil, E., Mehrasa, M., Jrgensen, B. N., and Catalão, J. P. S.: 'A Control Algorithm for the Stable Operation of Interfaced Converters in Microgrid Systems'. In: Proc. 5th IEEE PES Innovative Smart Grid Technologies (ISGT) European Conf.; 2014. p. 1-6.

[12] Katiraei, F., Iravani, M., R., and Lehn, P., W.: 'Small-signal dynamic model of a micro-grid including conventional and electronically interfaced distributed resources'. IET Gener. Transm. Distrib, 2007, 1, (3), pp. 369–378.

[13] Mohamed, Y.A-R.I., and El-Saadany, E.F.: 'Adaptive decentralized droop controller to preserve power sharing stability of paralleled inverters in distributed generation microgrids'. IEEE Trans. Power Electronic, 2008, 23, (6), pp. 2806–2816.

[14] Chung, I-Y., Liu, W., Cartes, D.A., Collins, Jr.E.G, and Moon, S-I.: 'Control methods of inverter-interfaced distributed generators in a microgrid system'. IEEE Trans. Industrial Electron, 2010, 46, (3), pp. 1078–1088.

[15] Ahmed, M.E-S., Orabi, M., and AbdelRahim, O.M.: 'Two-stage micro-grid inverter with high-voltage gain for photovoltaic applications'. IET Power Electron, 2013, 6, (9), pp. 1812–1821.

[16] Eghtedarpour, N., and Farjah, E.: 'Distributed charge/discharge control of energy storages in a renewable-energy-based DC micro-grid'. IET Renew. Power Gener, 2014, 8, (1), pp. 45–57.

[17] Khan, H., Dasouki, S., Sreeram, V., and Iu, H.H., and Mishra, Y.: 'Universal active and reactive power control of electronically interfaced distributed generation sources in virtual power plants operating in grid-connected and islanding modes'. IET Gener. Transm Distrib, 2013, 7, (8), pp. 885–897.

[18] Rokrok, E., and Golshan, M.E.H.: 'Adaptive voltage droop scheme for voltage source converters in an islanded multibus microgrid'. IET Gener. Transm Distrib, 2010, 4, (5), pp. 562–578.

[19] Planas, E., Gil-de-Muro, A., Andreu, J., Kortabarria, I., and Alegría, I.M.D.: 'Design and implementation of a droop control in d–q frame for islanded microgrids'. IET Renew. Power Gener, 2013, 7, (5), pp. 458–474.

[20] Kamel, R.M, Chaouachi, A., Nagasaka. K.: 'Enhancement of micro-grid performance during islanding mode using storage batteries and new fuzzy logic pitch angle controller'. Energy Conversion and Management, 2011, 52, (5), pp. 2204–2216.

[21] Radwan, A.A.A., and Mohamed, Y.A-R.I.: 'Modeling, analysis and stabilization of converter-fed AC microgrids with high penetration of converter-interfaced loads'. IEEE Trans. Smart Grid, 2012, 3, (3), pp. 1213–1225.

[22] Dasgupta, S., Mohan, S.N., Sahoo, S.K., and Panda, S.K.: 'Lyapunov Function-Based Current Controller to Control Active and Reactive Power Flow From a Renewable Energy Source to a Generalized Three-Phase Microgrid System'. IEEE Trans. Industrial Elects, 2013, 60, (2), pp. 799-813.

[23] Li, Y.W., and Kao, C-N.: 'An accurate power control strategy for power-electronic-interfaced distributed generation units operating in a low-voltage multibus microgrid'. IEEE Trans. Power Elects, 2009, 24, (12), pp. 2977-2987.

[24] Mehrizi-sani, A., and Iravani, R.: 'Potential-Function based control of a microgrid in islanded and grid-connected modes'. IEEE Trans. Power System, 2010, 25, (4), pp. 1883–1891.

[25] Guerrero, J.M., Chandorkar, M., Lee, T., and Loh, P.C.: 'Advanced Control Architectures for Intelligent Microgrids—Part I: Decentralized and Hierarchical Control'. IEEE Trans. Industrial Elects, 2013, 60, (4), pp. 1254–1262.

[26] Guerrero, J.M., Loh, P.C., Lee, T.L., and Chandorkar, M.: 'Advanced Control Architectures for Intelligent Microgrids—Part II: Power Quality, Energy Storage, and AC/DC Microgrids'. IEEE Trans. Industrial Elects, 2013, 60, (4), pp. 1263–1270.

[27] Etxeberriaa, A., Vechiua, I., Camblonga, H., Vinassab. J.M.: ‘Comparison of three topologies and controls of a hybrid energy storage system for microgrids’. Energy Conversion and Management, 2012, 54, (1), pp. 113–121.

[28] Wasiak, I., Pawelek, R., and Mienski, R.: ‘Energy storage application in low-voltage microgrids for energy management and power quality improvement’. IET Gener. Transm Distrib, 2014, 8, (3), pp. 463–472.

[29] Marquez, H.J.: ‘Nonlinear Control Systems, Analysis and Design’. John Wiley&Sons, 2003.

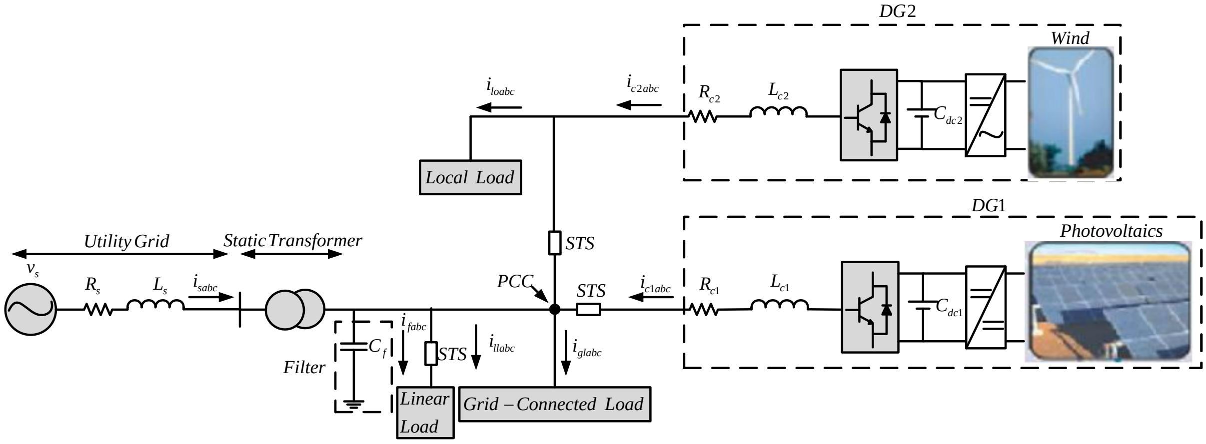

Fig. 1. General scheme of proposed microgrid model.

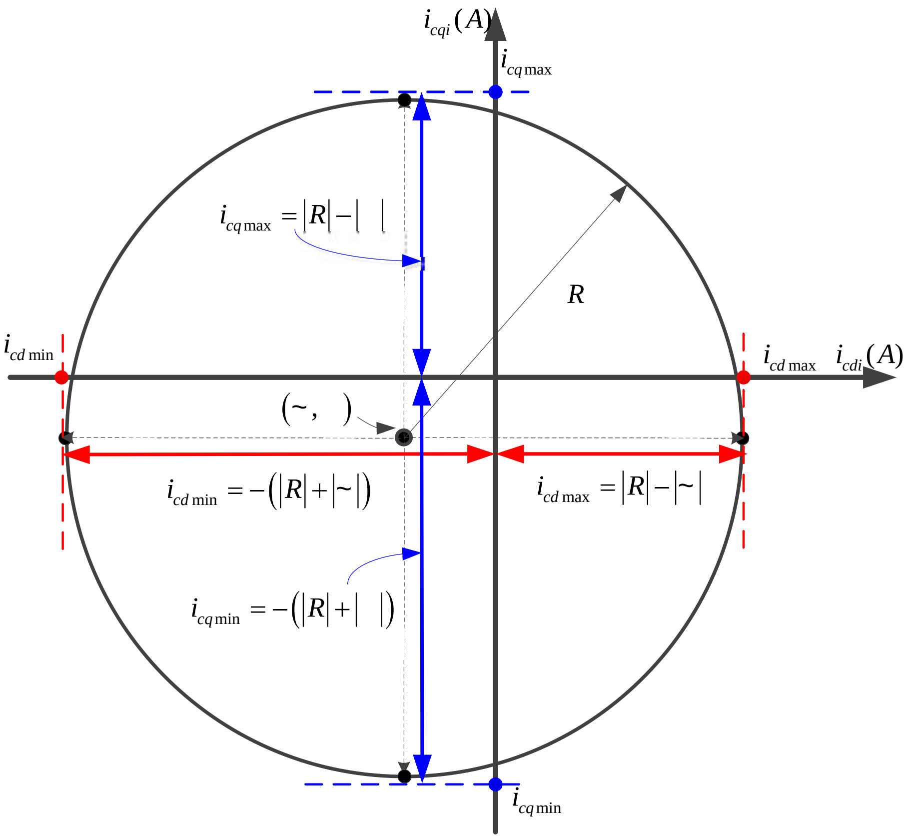

Fig. 2. $i_{cdi} - i_{cqi}$ **curve of DG units.**

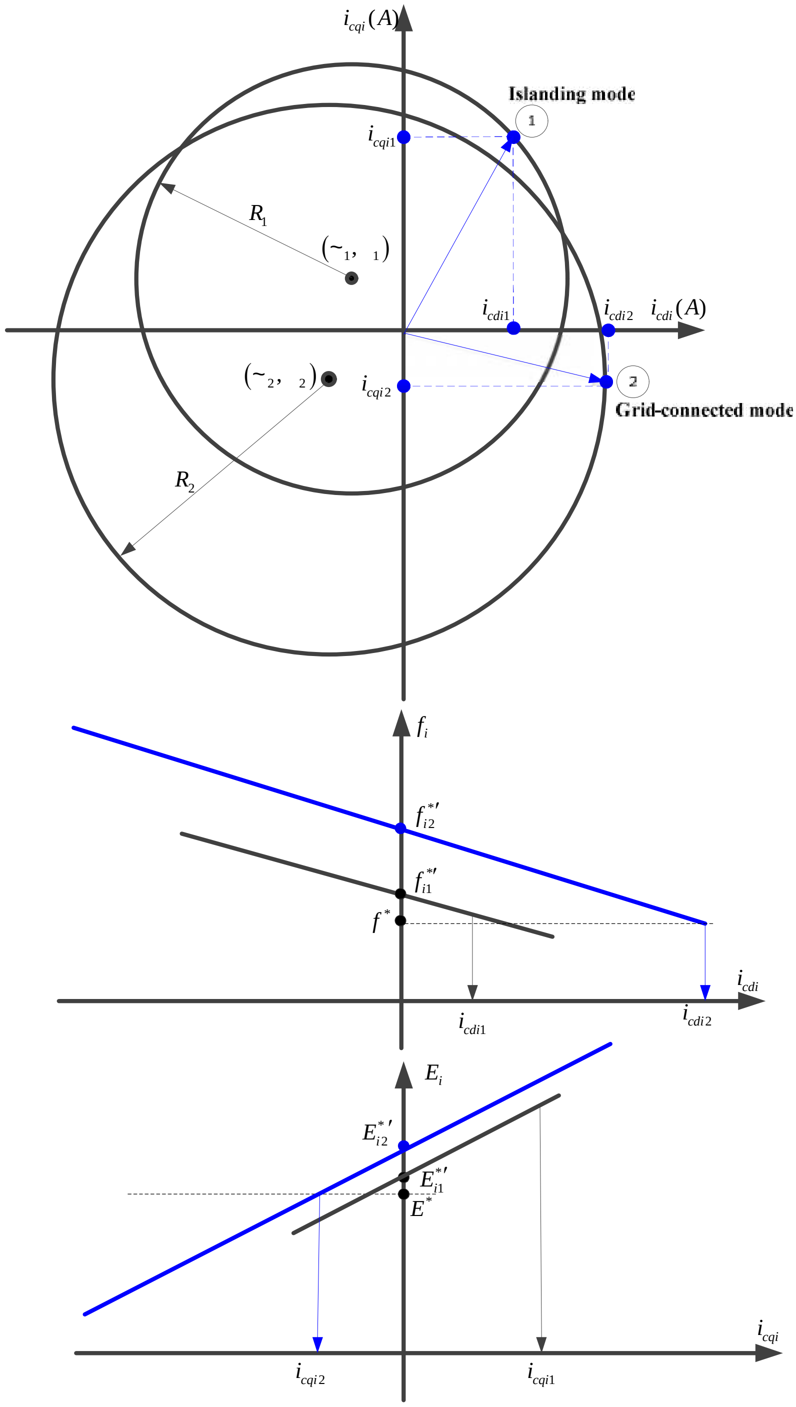

Fig. 3. The $i_{cdi} - i_{cqi}$, $i_{cdi} - f_i$ and $i_{cqi} - E_i$ curves of DG unit.

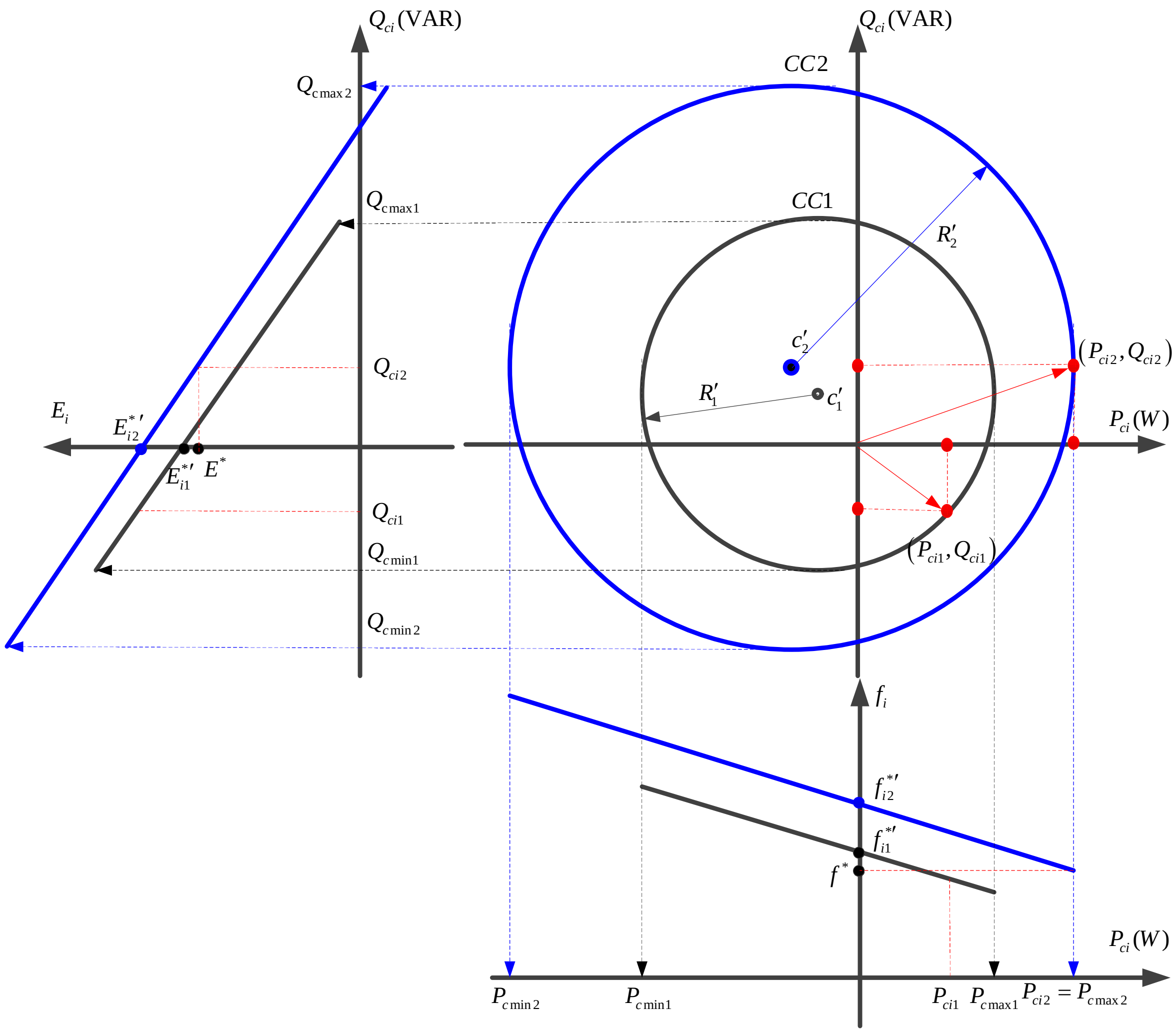

Fig. 4. The capability curve, $P_{ci} - f_i$ and $Q_{ci} - E_i$ droop control characteristics curves of DG unit.

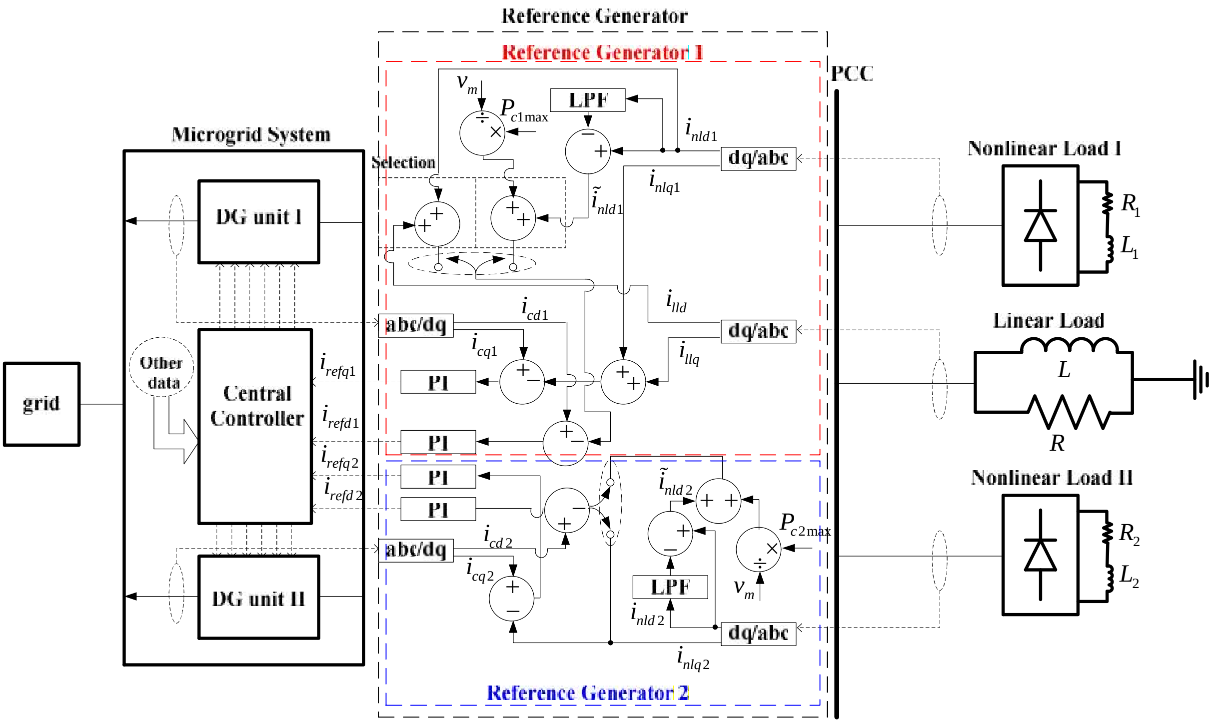

Fig. 5. Reference current components of DG units in d and q-axis.

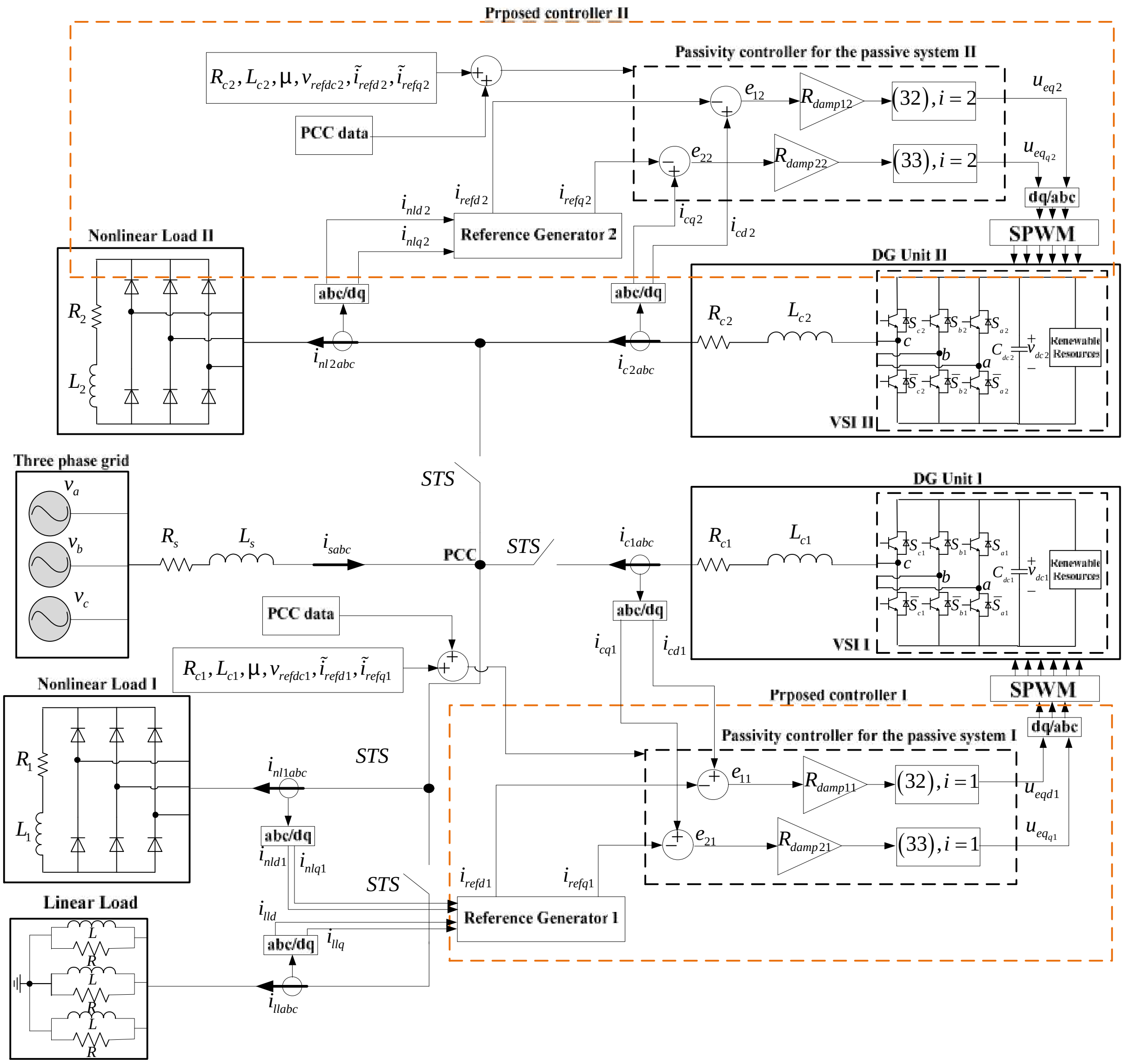

Fig. 6. Overall scheme diagram for the proposed model.

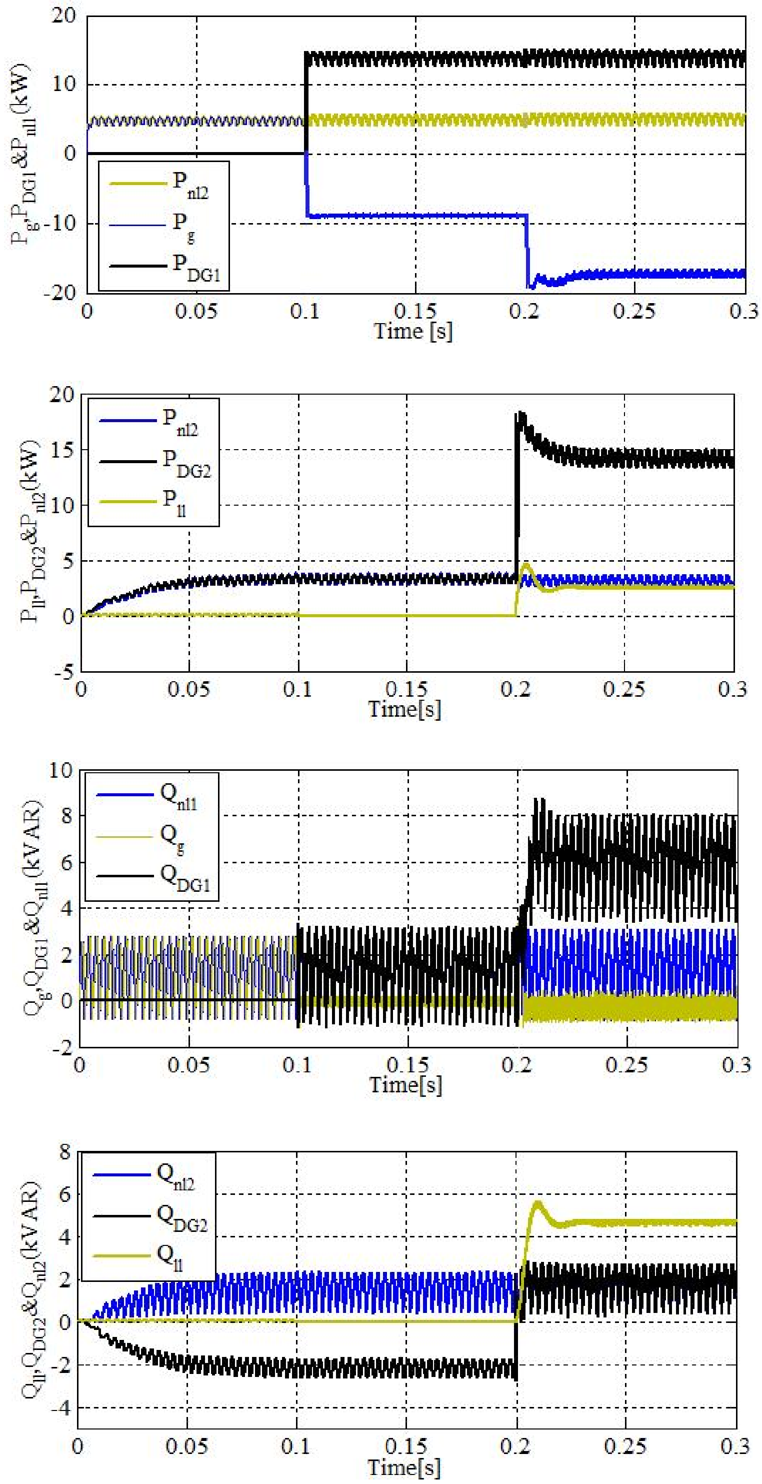

Fig. 7. (a) Active power sharing between grid, DG unit I, and nonlinear load I; (b) Active power sharing between linear load, DG unit II, and nonlinear load II; (c) Reactive power sharing between the grid, DG unit I, and nonlinear load I; (d) Reactive power sharing between the linear load, DG unit II, and nonlinear load II.

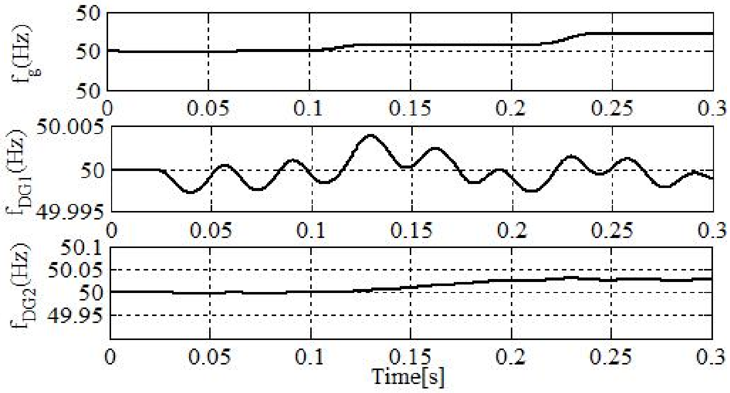

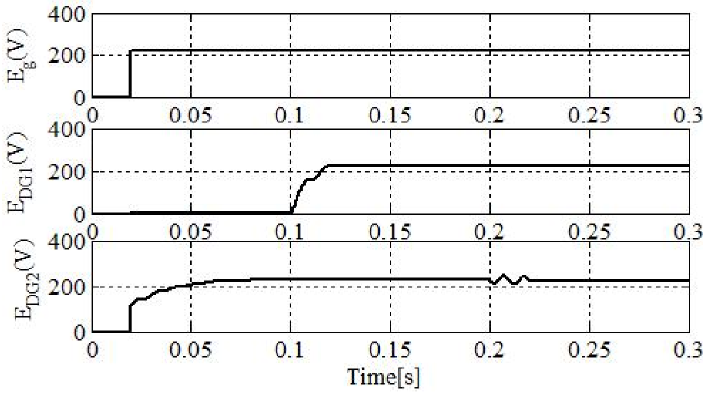

Fig. 8. (a) DG units output frequency and grid frequency; (b) Reactive power of linear load, DG unit II, and nonlinear load II.

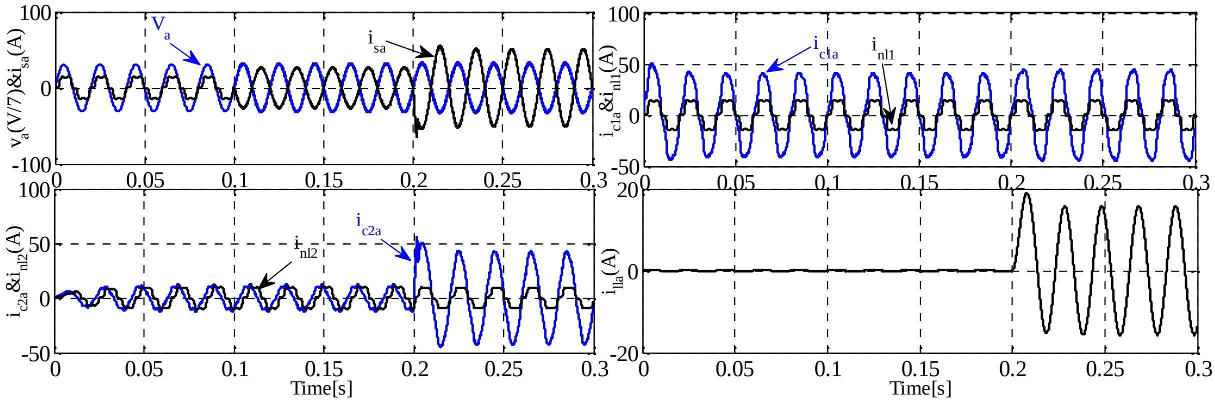

Fig. 9. DG units, grid, nonlinear and linear loads currents in phase "a"

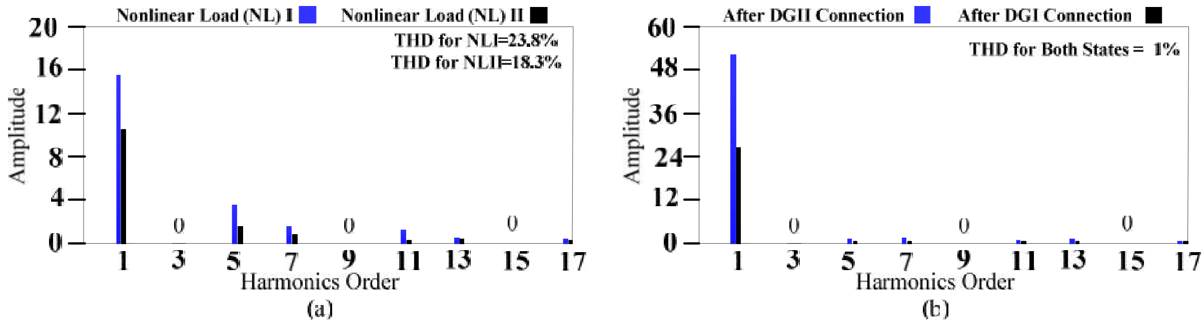

Fig. 10. The harmonic spectrum a) Nonlinear loads I&II currents b) the grid current (After DG I&II connection)